



OPEN

## Dexamethasone acetate loaded poly( $\epsilon$ -caprolactone) nanofibers for rat corneal chemical burn treatment

Da Ran Kim<sup>1,4</sup>, Sun-Kyoung Park<sup>1,4</sup>, Eun Jeong Kim<sup>1</sup>, Dong-Kyu Kim<sup>1</sup>, Young Chae Yoon<sup>1</sup>, David Myung<sup>2</sup>, Hyun Jong Lee<sup>3,4</sup> & Kyung-Sun Na<sup>1,4</sup>

Topical eye drop approaches to treat ocular inflammation in dry eyes often face limitations such as low efficiency and short duration of drug delivery. Nanofibers serve to overcome the limitation of the short duration of action of topical eye drops used against ocular inflammation in dry eyes. Several attempts to develop suitable nanofibers have been made; however, there is no ideal solution. Here, we developed polycaprolactone (PCL) nanofibers loaded with dexamethasone acetate (DEX), prepared by electrospinning, as a potential ocular drug delivery platform for corneal injury treatment. Thirty-nine Sprague Dawley rats (7 weeks old males) were divided into four treatment groups after alkaline burns of the cornea; negative control (no treatment group); dexamethasone eyedrops (DEX group); PCL fiber (PCL group); dexamethasone loaded PCL (PCL + DEX group). We evaluated therapeutic efficacy of PCL + DEX by examining the epithelial wound healing effect, the extent of corneal opacity and neovascularization. Additionally, various inflammatory factors, including IL-1 $\beta$ , were investigated through immunochemistry, western blot analysis, and quantitative real-time RT-PCR (qRT-PCR). PCL + DEX group showed histologically alleviated signs of corneal inflammation compared with DEX group, which showed a decrease in IL-1 $\beta$  and MMP9 in the corneal stroma. The quantitative expression on day 1 after alkaline burn of pro-inflammatory markers, including IL-1 $\beta$  and IL-6, in the PCL + DEX group was significantly lower than that in the DEX group. Notably, PCL + DEX treatment significantly suppressed neovascularization, and enhanced the anti-inflammatory function of DEX during the acute phase of ocular inflammation. Collectively, these findings suggest that PCL + DEX may be a promising approach to effective drug delivery in corneal burn injuries.

**Keywords** Dry eye, Dexamethasone eye drops, Nanofibers, Rats

The ocular surface is constantly exposed to the external environment, making it the most vulnerable tissue to external stimuli. Consequently, continuous inflammation and immune responses occur more often at the surface of cornea and conjunctiva than in other body parts. If inflammation or wound healing due to trauma, surgery, infection, or burns are not appropriately treated, corneal neovascularization and scar may cause irreversible fibrosis and vascularization, resulting in ocular pain and vision loss<sup>1,2</sup>. Topical steroids and cyclosporine A (CsA) are the most common treatment strategies used to control inflammation<sup>2,3</sup>. Moreover, in acute inflammatory conditions such as chemical or thermal burn, Stevens-Johnson syndrome, and ocular graft-versus-host disease, intensive treatment with steroid instillation every few minutes or hours are often mandatory<sup>4-6</sup>.

Topical eye drops, a representative topical drug delivery in the eye, are convenient and easy to apply, making them the most widely used drug form, especially for widespread ocular surface diseases<sup>7</sup>. However, the effect of the topical drugs on the ocular surface is time limited due to tear dilution, lacrimal turnover, blinking reflex, nasolacrimal drainage or ocular barriers<sup>8,9</sup>. Low ocular bioavailability of topically applied drug molecules can considerably limit their efficacy<sup>10</sup>. Therefore, there is an urgent need for a superior treatment delivery method that can provide more stable and continuous effect on the ocular surface.

<sup>1</sup>Department of Ophthalmology, Yeouido St. Mary's Hospital, College of Medicine, The Catholic University of Korea, 10, 63-Ro, Yeongdeungpo-Gu, Seoul 07345, Republic of Korea. <sup>2</sup>Byers Eye Institute at Stanford University School of Medicine, Palo Alto, CA 94303, USA. <sup>3</sup>Chemical and Biological Engineering, Gachon University, Seongnam-si, Gyeonggi-do 13120, Republic of Korea. <sup>4</sup>These authors contributed equally: Da Ran Kim, Sun-Kyoung Park, Hyun Jong Lee and Kyung-Sun Na. ✉email: hjee2@gachon.ac.kr; drna@catholic.ac.kr

Electrospun nanofibers have been extensively used in regenerative medicine for efficient drug delivery due to their rapid and easy fabrication and controllability of density and thickness by factors such as polymer solution concentration, flow rate, and voltage<sup>11,12</sup>. Electrospun nanofibers can be used as a drug delivery system to treat local lesions because of its advantage of high drug loading capacity, high drug encapsulation efficiency, and simultaneous delivery of diverse therapeutic agents<sup>13</sup>. Nanofibers loaded with triamcinolone acetonide, an anti-inflammatory drug, reduced inflammation in rat experimental autoimmune uveitis<sup>14</sup>. Furthermore, a previous study has reported that CsA-loaded nanofibers transferred onto the ocular surface injured with alkali could represent an effective alternative mode of therapy for reducing inflammation and further damage<sup>15</sup>. Nanofibers made of poly ( $\epsilon$ -caprolactone) (PCL) and dexamethasone (DEX) acetate were developed to deliver corticosteroids to the back of the eye during the post-operative period of any vitreoretinal disease<sup>13</sup>. Electrospun fiber with gelatin and PCL mixture in a rabbit organ culture model showed that the fiber was able to support wound healing in the cornea<sup>16</sup>. Although there have been cases where DEX has been incorporated into electrospun fibers and used in drug delivery systems, there has been no relevant study on alkali burn treatment. Therefore, we aimed to evaluate the usefulness of PCL nanofibers with encapsulated DEX for the treatment of alkali-injured cornea in rats.

## Results

### Morphological characterization of electrospun nanofibers in vitro

To develop a drug delivery platform appropriate for ocular application, we first manufactured PCL nanofibers incorporating dexamethasone acetate using electrospinning techniques. The electrospun PCL fibers were prepared in two formulations, PCL (13 wt%) or the PCL:DEX blend (13:5 wt%), respectively. Morphological analysis conducted with a scanning electron microscope (SEM) showed the structure of the nanofibers (Fig. 1A,B). The average diameter of the nanofibers was determined to be  $1.79 \pm 0.14 \mu\text{m}$  for the 13 wt% PCL fibers and  $1.76 \pm 0.13 \mu\text{m}$  for the PCL:DEX (13:5 wt%) fibers (Fig. 1C), indicating no significant morphological differences between the PCL fibers with and without the drug.

### Release profile of Rhodamine 6G from the PCL nanofibers in vitro

Next, we assessed the drug release profile from PCL nanofibers with time using Rhodamine 6G as a fluorescent tracer. The release patterns of Rhodamine 6G from the fibers are shown in Fig. 2. Macroscopic observation revealed a noticeable change in the appearance of the fibers over time (Fig. 2A). An intense dark red color due to presence of Rhodamine 6G gradually changed to a pale pink color within the first hour after release, and the color became significantly lighter after 6 h (Fig. 2A,B). Quantitatively analysis revealed that more than 80% of the fluorescent tracer was rapidly released from the PCL fiber within the first 20 min (Fig. 2B). These results indicate that our PCL nanofibers could serve as a potential system for drug delivery.

### Effect of drug delivery from PCL fiber on corneal epithelial wound healing after alkali burn in vivo

To evaluate the role and importance of re-epithelialization in corneal wound healing, fluorescein dye staining was utilized on the corneal surface to visualize the wounds or defects of the epithelium; further, we examined whether regeneration is facilitated by DEX-loaded PCL nanofibers. The extent of corneal erosion was monitored across all experimental groups for 7 days following chemical injury (Fig. 3A). Although a gradual decrease in the

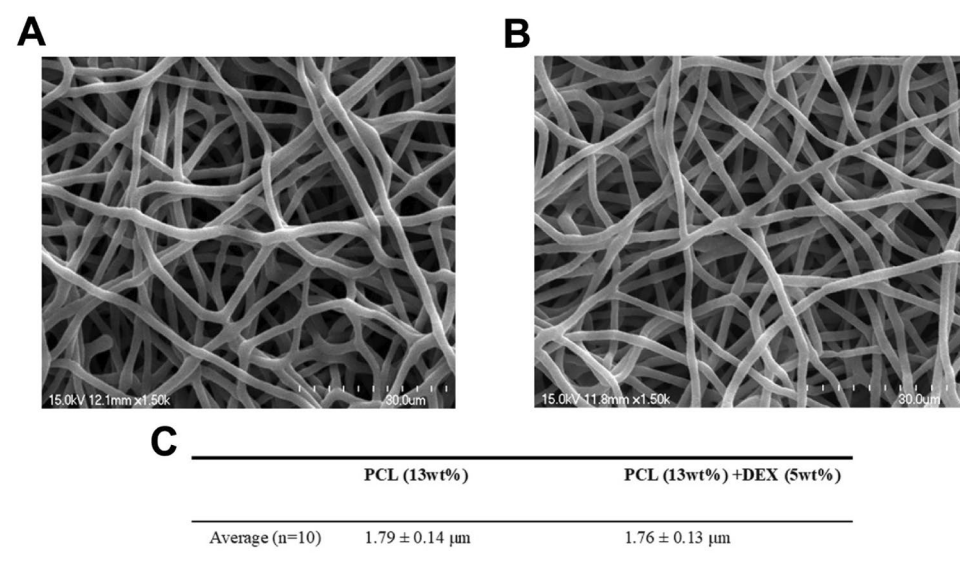


**Figure 1.** Morphological characterization of electrospun nanofibers in vitro. (A, B) SEM images of PCL (A) and PCL + DEX fiber (B). Scale bars, 30  $\mu\text{m}$ . (C) The average diameter of PCL and PCL + DEX fiber.

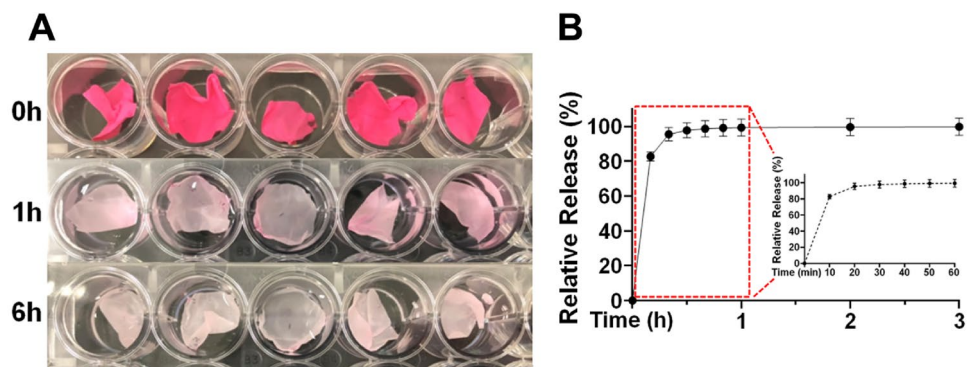


**Figure 2.** Release profile of Rhodamine 6G from the PCL nanofibers in vitro. **(A)** Photographic images of Rhodamine 6G released from the nanofibers. **(B)** Time courses of relative release of Rhodamine 6G from PCL fibers was quantitatively analyzed. Red dot box indicated percentage of relative release within 1 h.

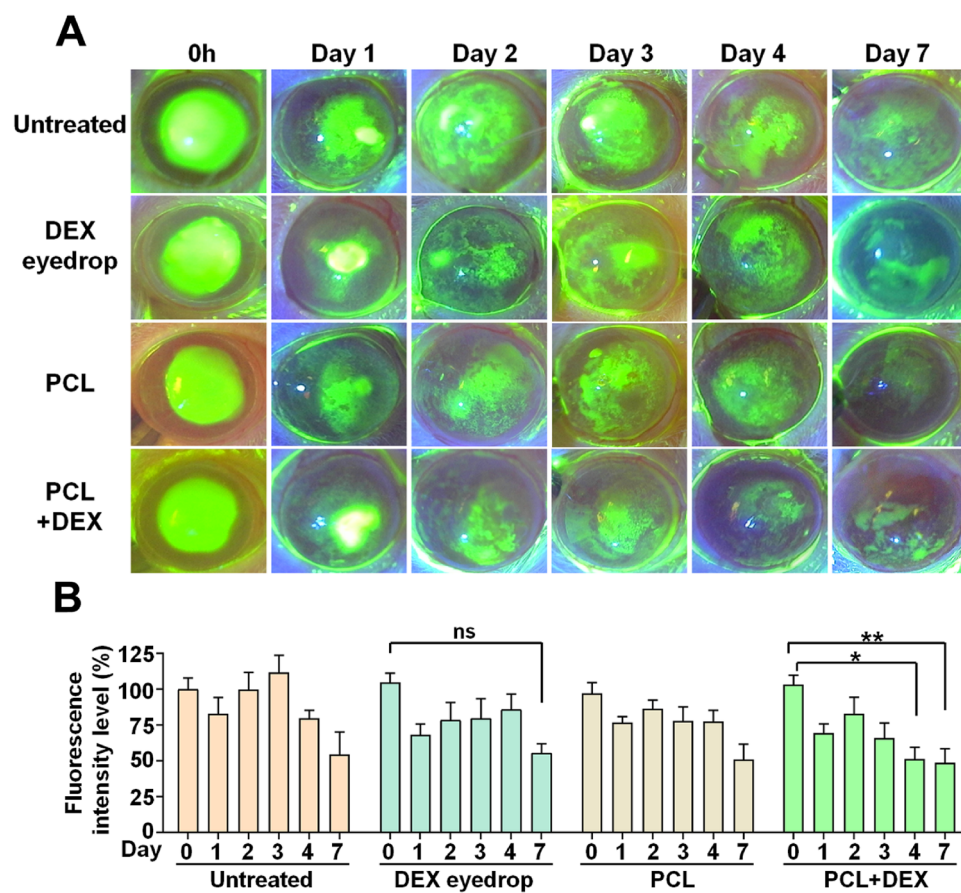


**Figure 3.** Effect of drug delivery from PCL fiber on corneal epithelial wound healing after alkali burn in vivo. **(A)** Representative slit-lamp images of corneal fluorescein staining between the four respective groups at time dependent after alkali burn. **(B)** Changes in the intensity of fluorescence at the different days among the four groups after alkali burn. Six additional animals were analyzed in each group. All values are presented as the mean  $\pm$  SEM (ns: not significant, \* $p < 0.05$ , \*\* $p < 0.01$ ). Statistical significance was determined by two way ANOVA with Tukey's post hoc comparison between groups.

degree of corneal erosion was observed over time in all groups, there was no significant difference in the extent of erosion between groups (Supplementary Fig. 1). However, treatment with PCL + DEX significantly reduced the intensity of fluorescence starting from day 4, indicative of enhanced re-epithelialization; whereas the group treated with DEX-eye drop showed no significant change in fluorescence intensity during all period (Fig. 3B). These results suggest the better ability of PCL + DEX system with respect to corneal re-epithelialization post-chemical damage, compared with the general eye drops treatment.

### Comparison of the degree of corneal opacity and neovascularization (NV) in the injured and treated groups following a clinical grading system

To evaluate the impact of a drug delivery system on corneal inflammation following an alkali burn in rat models, we analyzed the degree of corneal opacity and neovascularization (NV) in different groups: untreated (injured), DEX eye drop, PCL nanofiber, and PCL + DEX treated groups. To reduce subjective bias, corneal specialists (D.R.K., S.K.P., Y.C.Y., and K.S.N) randomly observed the photographs and graded them through a blind test. Macroscopic imaging conducted on day 7 post-chemical damage exhibited significant increase in the NV area of the untreated and DEX eye drop groups, as evidenced by the increasing mean values of corneal NV grading. On the contrary, the distribution and associated rating of corneal NV were markedly reduced in groups treated with PCL + DEX than in the other groups (Fig. 4A,B). Moreover, the scores for the PCL + DEX treated groups seemed to be lower than those in other groups when we analyzed the mean value of corneal opacity grading for each group on day 7 after injury, although the change did not show statistical significance (Fig. 4A,C).

### Verification of treatment efficacy of inflammation-related factors of PCL + DEX nanofibers after chemical damage

We performed further validation of the therapeutic efficacy of PCL + DEX nanofibers through hematoxylin & eosin (H & E) staining of tissue and immunohistochemical (IHC) analysis for fibrosis or inflammation-related

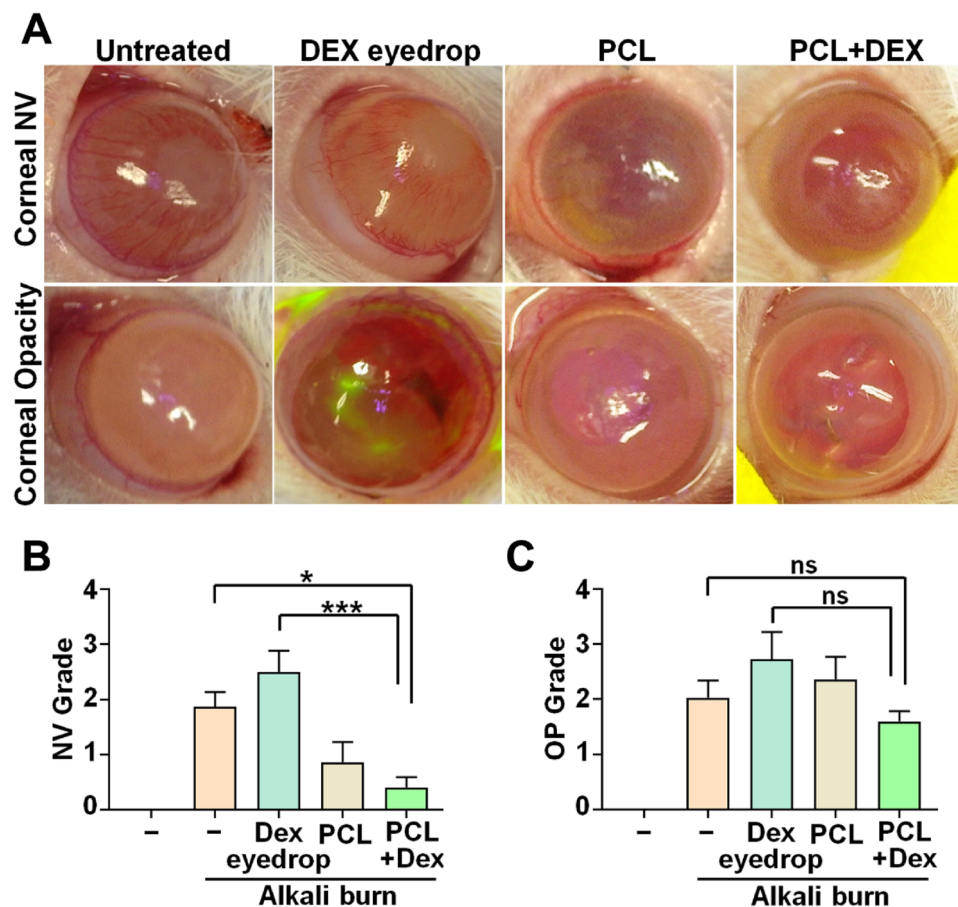


**Figure 4.** Comparison of the degree of corneal opacity and neovascularization (NV) in the injured and treated groups following a clinical grading system. (A) Representative slit-lamp images showing differences in corneal opacity and NV among the five different groups on day 7 after alkali burn. (B, C) Quantification of the grade in corneal opacity (B) and NV (C) of each group. All assessment were evaluated by blind-review at least six rats in each group. All values are represented as the mean  $\pm$  SEM (ns: not significant,  $*p < 0.05$ ,  $***p < 0.001$ ). Statistical significance was analyzed using one-way ANOVA with Tukey's post hoc comparison between groups.

markers of the same group. H & E staining results indicated that untreated corneas had looser stromal collagen structure than did the groups treated with DEX eye drop, PCL, and DEX + PCL (Fig. 5). Moreover, the expression levels of MMP9 and IL-1 $\beta$  were significantly reduced in the PCL + DEX groups than in the untreated or DEX eye drop groups (Fig. 5B,C). However, immunohistochemical staining revealed no significant difference in the expression of  $\alpha$ -SMA among all groups (Fig. 5D).

In addition to histological analyses, we investigated the expression of several proteins associated with inflammation and angiogenesis, including MK2, IL-1 $\beta$ , TGF $\beta$ 1, TGF $\beta$ 2, VEGF and VEGF-A, in cornea samples obtained from the respective groups. There were no significant differences in the levels of MK2, IL-1 $\beta$ , TGF $\beta$ 1, TGF $\beta$ 2, VEGF, and VEGF-A across all groups (Fig. 6). Nevertheless, a tendency towards lower VEGF protein expression was observed in the PCL + DEX-treated group, in line with the clinical analysis findings revealing that angiogenesis was suppressed (Fig. 6E).

In the short-term qPCR analysis, the expression of IL-6 was significantly reduced in the DEX + PCL group than in the other groups on day 1 after injury. In the case of IL-1 $\beta$ , the expression was considerably lower in PCL + DEX on day 1 after injury; however, over time, it was relatively higher than in the DEX group (Fig. 7). Taken together, these findings suggest that the application of DEX-loaded PCL nanofibers after chemical damage can effectively mitigate signs of corneal inflammation and reduce neovascularization, without significant adverse effects on the expression levels of inflammatory factors.

## Discussion

Multiple studies have shown PCL fibers to be promising ocular delivery platforms due to their remarkable properties, including high kinetic and thermodynamic stability, biocompatibility, and biodegradability<sup>17–21</sup>. Various drug-loaded PCL fibers prepared from solution, suspension, and emulsion have demonstrated the potential of PCL fibers as a drug delivery option for any type of drug<sup>22–24</sup>. These fibers can also be prepared

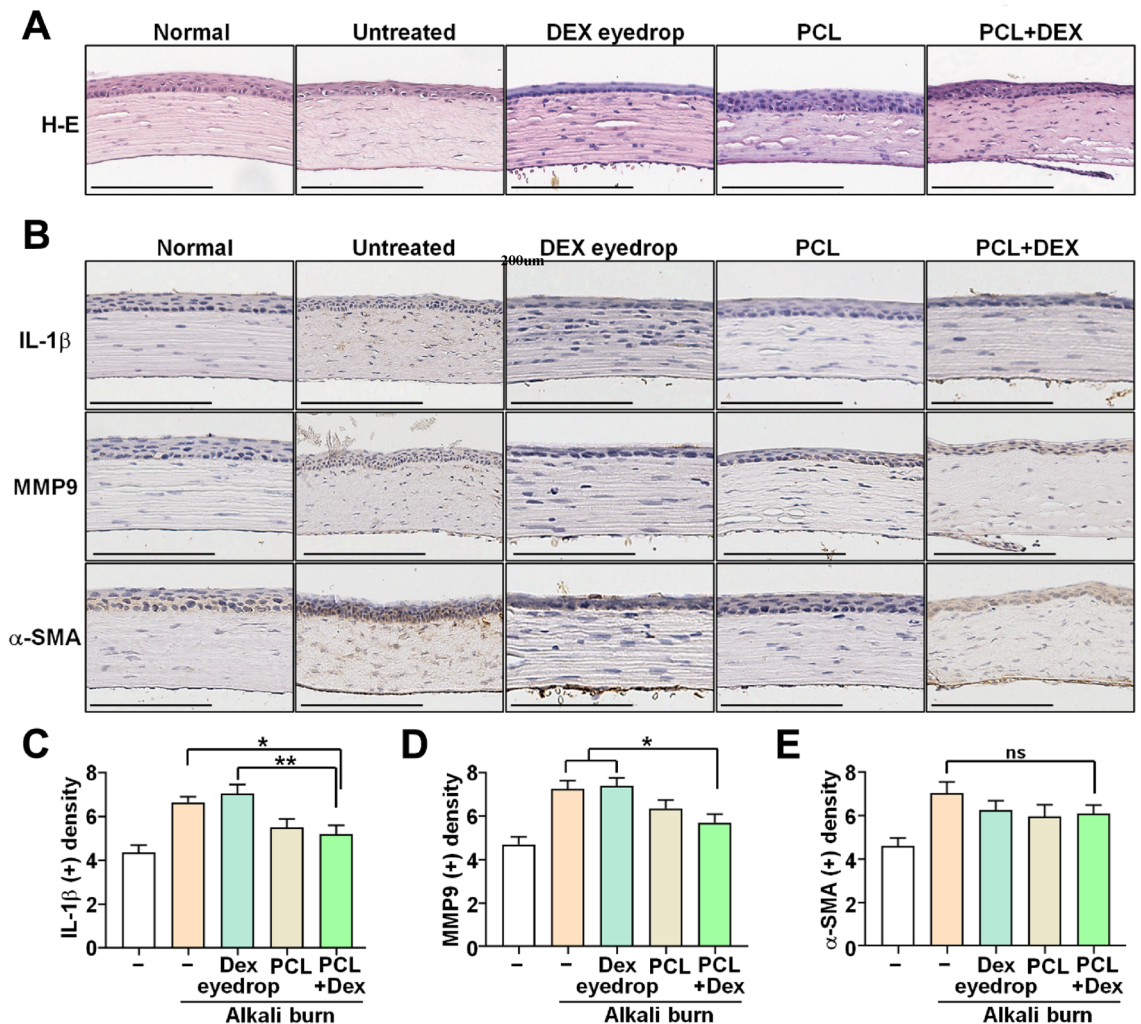


**Figure 5.** Analysis of the infiltration and density of inflammatory factors into the corneal stroma. (A) Representative images H & E and (B–E) immunohistochemistry (IHC) staining on day 7 after alkali burn. Scale bars: 200  $\mu$ m. All data are represented as the mean  $\pm$  SEM (ns: not significant, \* $p$  < 0.05, \*\* $p$  < 0.01). Statistical significance was analyzed using one-way ANOVA with Tukey's post hoc comparison between groups.

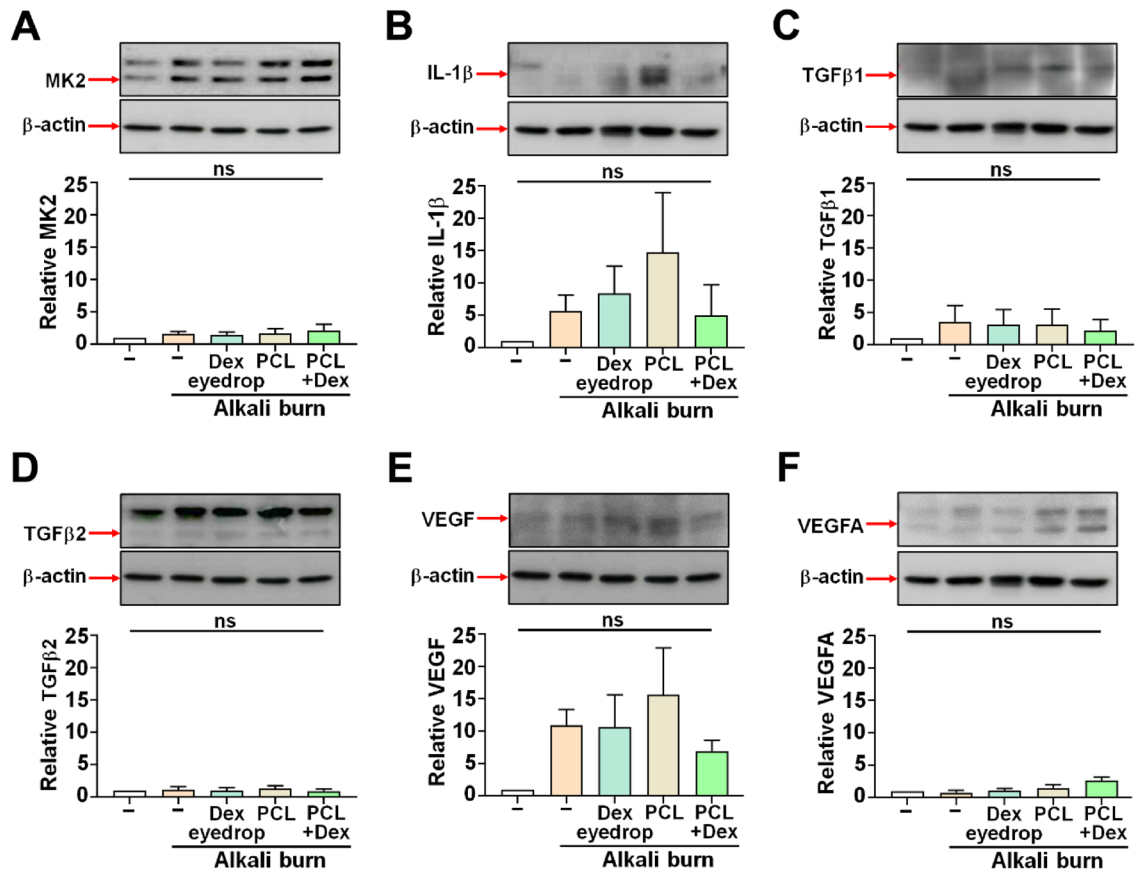


**Figure 6.** Representative western blot images of specific proteins associated with inflammation and angiogenesis on day 7 after alkali burn. (A–F) Expression levels of each protein were measured by immunoblotting. The quantified band of specific protein is indicated as the red arrow on the left side of the blot. The data were normalized to total  $\beta$ -actin expression,  $N = 3$ . All values are represented as mean  $\pm$  SEM (ns: not significant). Statistical significance was determined by one-way ANOVA with Tukey’s post hoc comparison between groups.

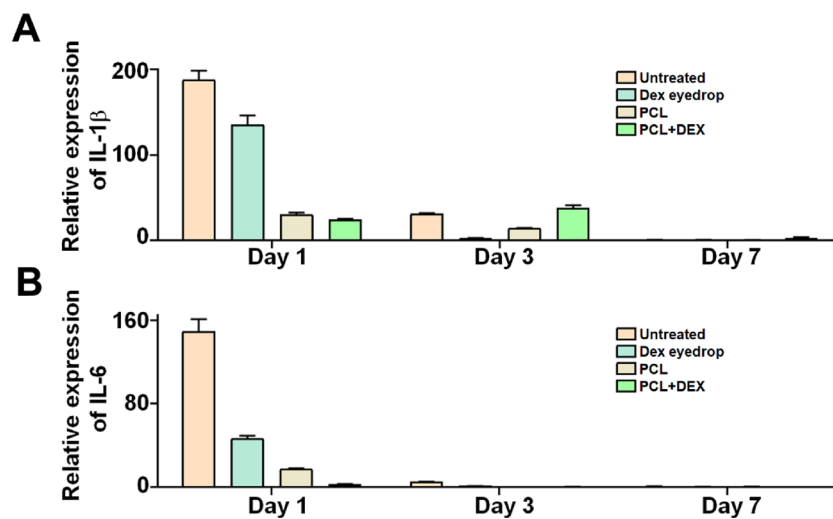


**Figure 7.** Expression levels of IL-6 and IL-1 $\beta$  genes measured by quantitative real-time PCR with day 7 after alkali burn. IL-6 and IL-1 $\beta$  levels greatly reduced in groups treated PCL + DEX compared with those in the untreated or DEX eye drop groups. All data are presented as mean  $\pm$  SEM. Statistical significance was calculated by two-way ANOVA with Tukey’s post hoc comparison between groups.

after co-polymerization with other polymers such as PEG, chitosan, or chlorophyllin; some researchers have investigated polymer combinations in recent years<sup>25–28</sup>. However, most of the previous studies have been in vitro or ex vivo studies introducing characteristics of the materials or evaluating drug release profiles. There have been no in vivo studies evaluating the therapeutic effects of drug-loaded PCL fibers using rat models with corneal chemical burns. Accordingly, in this study, we prepared a PCL fiber mixed with dexamethasone acetate by electrospinning technique and attempted to study the therapeutic effects of the fibers on a rat model with corneal chemical burns.

Steroids are known to inhibit the re-epithelialization of the cornea<sup>29–31</sup>. Our results showed no significant differences in re-epithelialization between different groups after alkali burn. Nevertheless, treatment of PCL + DEX improved the corneal epithelial wound healing over time than did conventional DEX eyedrops. In addition, PCL itself did not have a negative effect on the re-epithelialization of the cornea, suggesting the capability of PCL fibers to deliver the drug to the cornea.

The mean grading value of neovascularization was significantly lower in the PCL + DEX group than in the DEX eye drop group. We identified that PCL + DEX had a tendency for better corneal neovascular inhibition effect than did DEX eyedrops. The mean grading value of the neovascularization was lower in the group treated with PCL than in the untreated or DEX eye drop group, suggesting that PCL itself did not cause corneal neovascularization by irritation or inflammation. Meanwhile, no significant differences were noted in corneal opacity among different groups. In the process of wound healing and tissue repair, mature myofibroblasts secrete collagens and extracellular matrix materials that form fibrotic scars<sup>32</sup>. However, the therapeutic effect of PCL + DEX may have been insufficient to suppress corneal opacity as the process takes weeks to years; therefore, our analyzed period of 7 days may have been too short to observe the differences between groups. This can be confirmed in the results of in vitro drug release studies, in which the drug release time was short, as shown in Fig. 2.

In the eye, pro-inflammatory cytokine IL-1 activity is correlated with corneal neovascularization<sup>33,34</sup>, and expression of IL-1 $\beta$  in the cornea is increased in various corneal diseases and other complications such as chemical burns<sup>35</sup>. Especially, dexamethasone inhibits IL-1 $\beta$ -induced neovascularization and the expression of the angiogenesis-related factors<sup>36</sup>. MMP9 production is stimulated by the IL-1 $\beta$ , and these factors play a role in corneal matrix degradation<sup>37</sup>. Hence, the expression of MMP9 and IL-1 $\beta$  in the anterior stroma is associated with inflammation. Consistent with H & E staining results, IHC staining revealed that the expression of MMP9 and IL-1 $\beta$  was greater in the corneas treated with DEX eyedrops than in those treated with PCL + DEX. Our results showed that the expression of MMP9 and IL-1 $\beta$  was detected less in PCL + DEX-treated corneas than in the DEX eye drop-treated corneas. These results imply that PCL + DEX is superior to DEX eyedrops in controlling the angiogenesis and inflammation of the cornea. Meanwhile, corneas treated with PCL showed a compact collagen structure similar to those treated with PCL + DEX fiber, suggesting that PCL fiber did not show negative effects related to fibrosis or inflammation in the process of wound healing and tissue repair for corneal alkali burn.

$\alpha$ -SMA is used as a marker of activated myofibroblasts, and  $\alpha$ -SMA expression implies activated fibrosis in the corneal stroma<sup>32</sup>. IHC staining showed that  $\alpha$ -SMA expression in PCL + DEX group was lower than the untreated group, and was similar to that in the DEX eye drop group, but there was no statistical difference between groups.

Western blot analysis revealed no statistically significant differences between the groups. However, the expression levels of IL-1 $\beta$  and VEGF tended to be lower in corneas treated with PCL + DEX than in those treated with DEX eyedrops, despite the large variation between individuals. We identified that PCL + DEX was superior to DEX eyedrops in terms of anti-inflammatory and neovascular suppression. Meanwhile, these factors were randomly expressed in the corneas treated with PCL fiber without a specific trend. We assumed that PCL fibers did not show a positive or negative effect consistently in terms of inflammation or neovascularization in the cornea.

To confirm a more immediate anti-inflammatory response and changes over time after the injury, qPCR was additionally performed on days 1, 3, and 7. IL-1 $\beta$  and IL-6 are known to serve as proinflammatory cytokines, especially as angiogenic activities in the acute phase of ocular inflammation<sup>38,39</sup>. DEX regulates inflammation by inhibiting the action of these cytokines<sup>40</sup>. In our study, the anti-inflammatory function of DEX observed in the acute phase of ocular inflammation appears to be significantly improved on day 1 in the PCL + DEX group.

There are few limitations to this study. First, the number of animals used was small and statistical significance could not be observed in some results. Instead, we estimated the relative superiority in therapeutic effects by analyzing trends between groups. Therefore, it is necessary to conduct additional experiments under the same conditions in future studies to confirm the reproducibility and consistency of the results and examine statistical significance. Second, despite suturing the eyelids, the fibers might unexpectedly fall off early due to eyelid tension or blinking rate, which can serve as variables on the residence time of the fibers. After the damage occurred, each nanofiber was injected into the fornix and lateral 1/3 of the eyelid was sutured, but we were unable to identify PCL nanofibers in all PCL and PCL + DEX groups when examined the day after the treatment. It is unclear whether the fibers melted or could not be detected, but we were not able to rule out the possibility that it fell off early. However, as nearly 80% of the drug is released from the fibers within 20 min, it is unlikely that it would have affected the experimental results even if it fell off in the middle of the study. In clinical settings in human, we may perform eyelid closure with simple taping or pressure patch, or therapeutic soft contact lenses can be used instead of invasive eyelid suture. Third, the observation period was relatively short. In case of corneal alkali burns, complications such as corneal opacity and neovascularization progress over several weeks to months; therefore, 7 days is a short period and differences between groups may occur. In the future, it is necessary to conduct studies by extending the observation period to compare the long-term therapeutic efficacy in the process of tissue repair. Fourth, the action time of the drug was too short as nearly 100% of the drug was released within 1 h after showing an initial burst for 20 min. Despite the short action time, PCL + DEX showed superiority in inhibiting corneal neovascularization than did DEX eyedrops on day 7 after burns.

As corneal remodeling takes place over several weeks to months, we can expect a better long-term prognosis if we use an effective drug delivery substance with a longer action time together. Typically, a matrix type of drug

delivery system exhibits a high initial drug release, followed by a decreased release rate due to the increasing diffusion distance from the drug molecules inside to the surface<sup>41</sup>. The drug release rate can be modulated by altering fabrication parameters such as the concentration of polymer and drug, type of solvent, or electrospinning conditions. The concentration of polymer and drug affects the fiber diameter, drug encapsulation, and tensile strength<sup>27,42,43</sup>. A more sustained release is observed when the molecular weight of the drug is high<sup>44</sup>. Therefore, in future studies, PCL fibers with a longer residence time on the ocular surface can be prepared by mixing different ratios of PCL and DEX or loading other steroids such as loteprednol etabonate, fluocinolone acetonide, or difluprednate with a higher molecular weight than dexamethasone acetate. However, it will be necessary to identify a ratio of PCL and steroids with optimal residence time, considering that steroids can cause infection or inhibit corneal re-epithelialization.

Nevertheless, this study is valuable as it is the first *in vivo* study to examine the therapeutic effects of steroids-loaded PCL fibers in various clinical aspects such as corneal re-epithelialization, opacity, and neovascularization and ascertain the possibility of PCL fibers as a drug delivery system on corneal alkali burns in rat model. Additionally, placing the fibers in the fornix has advantages in that it is less invasive and easier to apply in clinical practice compared with injecting fiber into the subconjunctival area<sup>19,20</sup>, anterior chamber<sup>45</sup>, or vitreous cavity<sup>13,46</sup>. However, although nanofibers can be easily applied to the eye, they can fall off just as easily. To increase the bioavailability of the sutureless drug-loaded PCL fibers, it is necessary to develop strategies to ensure that the fibers stay inside the cornea during the drug action time. The fiber can be fabricated to have cations or a similar structure with the corneal epithelial cell's microvilli. These strategies take advantage of the negatively charged ocular surface to increase their precorneal residence time through electrostatic interactions, and strengthen the adhesion with ocular surface by increasing the friction force, respectively. Further, the fibers can be fabricated in a ring shape with biocompatible metallic ring on a rim to preserve visual axis. This can exhibit the advantage of securing its position by placing the upper and lower parts in fornix without interfering with the vision.

Although further research is required, the drug delivery system using PCL can be easily applied to the eye, and has been shown to effectively increase the efficacy of loaded dexamethasone without causing adverse effects. We expect that in the future, this approach will be able to make a great contribution to improving the simple and long-lasting effects of eye drops in clinical practice.

## Conclusions

Although there were no statistical differences, we identified that PCL + DEX had a greater therapeutic effect than DEX eye drop in terms of anti-inflammation in the initial treatment of corneal alkali burns within 7 days. In particular, it was shown to maximize the anti-inflammatory function of DEX in acute inflammation. Based on these results, we conclude that rapid control of inflammation with an initial application of drugs within 20 min before the chemicals penetrate the corneal stroma and cause inflammation throughout the cornea is a key aspect that determines the prognosis of the disease.

## Materials and methods

### Fabrication of PCL fiber

Unless otherwise noted, all chemicals and solvents were used as provided by the manufacturers. PCL (MW 80,000), 2,2,2-trifluoroethanol (TFE), Rhodamine 6G, and DEX were acquired from Sigma-Aldrich (St. Louis, MO, USA). Phosphate-buffered saline (PBS; pH 7.4) was purchased from Thermo Fisher Scientific (Waltham, MA, USA).

To fabricate PCL fiber, PCL was dissolved in TFE as 13 wt%, and DEX was added to 5 wt% of the total solution. The polymer solution was filled into a syringe and ejected through a 23G needle. The flow rate, voltage, and run time of electrospinning were 1.5 mL/h, 16.0 kV, and 1 h, respectively. The distance between the needle tip and the collector was 10 cm (Fig. 8).

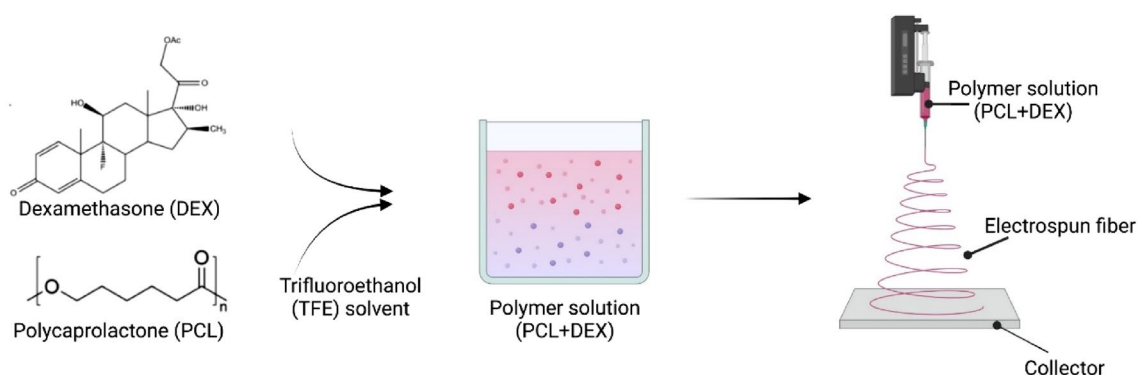


**Figure 8.** Schematic illustration for the preparation of DEX + PCL electrospun fiber.



### Scanning electron microscope

Scanning electron microscope (SEM) photographs were obtained using an SEM (SU8600, Hitachi, Japan) at the Smart Materials Research Center for IoT, Gachon University, Korea. All samples were attached to a brass sample holder with double-sided adhesive tape and sputter-coated with gold to make them electrically conductive.

### In vitro release profile

Rhodamine 6G was added to quantify the release profile from PCL electrospun fibers. Rhodamine 6G was added to 5 wt% of the total solution, and the electrospinning was performed in the same condition. Rhodamine 6G release was carried out in 24-well plates by immersing each scaffold in 2 mL of PBS. At each point, the entire solution of each well was removed and stored, and then PBS was added to each well. The fluorescence intensity of the stored solution was measured using Nanodrop (BioTek, Winooski, VT, USA) and the intensity was converted to concentration via the fluorescence intensity standard curve.

### Animals and corneal alkali burn model

Experimental protocols and animal care were performed according to the guidelines for the care and use of animals established by Yeouido St. Mary's Hospital and complied with the ARRIVE guidelines. The Animal Experimentation Ethics Committee of Yeouido St. Mary's Hospital approved the experimental protocols (approval number: YEO-2021-012FA, YEO-2022-008FA). Overall, 33 male Sprague Dawley (SD) rats (7 weeks old, 200–300 g) were purchased from Saerobio Inc. Anesthesia was achieved by intraperitoneal injection of ketamine hydrochloride (30 mg/kg). Alkali burn injury was performed on the right eye and was induced by pressing a qualitative filter paper disc (3.0 mm in diameter, Hyundal micro) containing 1 N NaOH onto the central cornea for 30 s. After removal of the filter paper disc, the corneal surface was carefully rinsed with 50 mL of physiological saline solution for 5 min. Study protocols were reviewed and approved by the Institutional Animal Care and Use Committee (IACUC) of the Catholic University of Korea (IRB No: YEO-2020-004FA), and this study was conducted in compliance with Animal Welfare Regulations. The animals were randomly divided into four groups (n = 5–9 per group). Sample size requirement estimates were based on clinical examination scores and testing at the study endpoint. In the first group of animals, no further treatment was applied to the injured eyes (control group). In the second group, DEX eyedrops were applied onto the injured corneal surface (DEX group). In the third group, PCL fibers were cut into approximately 1 × 1 mm sizes and implanted into the lower fornix (PCL group). In the fourth group, DEX/PCL fibers were cut into approximately 1 × 1 mm sizes and implanted into the lower fornix (DEX/PCL group) (Fig. 9). In all animals, the outer third of the upper and lower eyelids were sutured to prevent the PCL from falling off. (Fig. 9). DEX eyedrops were applied once daily to all experimental groups except for one group of the normal and negative control. Photographs of the corneas were captured on days 0, 1, 2, 3, 4, and 7 post injury. Animals were sacrificed on day 7 after alkali burn. The experimental eyes were enucleated and embedded within a mold. Healthy corneas served as controls.

Six other male SD rats of the same model were prepared for a short-term effect evolution. Anesthesia and alkaline burns were performed in the same manner as described above, except for those performed on both eyes. The eyes were randomly divided into four groups (n = 3 per group). In the first group of eyes, no further treatment was applied to the injured eyes. In the second group, DEX eyedrops were applied onto the injured corneal surface. In the third group, PCL fibers were cut into approximately 1 × 1 mm sizes and implanted into the lower fornix. In the fourth group, DEX/PCL fibers were cut into approximately 1 × 1 mm sizes and implanted into the lower fornix (Fig. 9). In all animals, the outer third of the upper and lower eyelids were sutured (Fig. 9). DEX eyedrops were applied once daily in all experimental groups except for one group of the normal and negative control. Animals were sacrificed on day 1, 3, or 7 after alkali burn and the eyeballs were dissected for separation of corneal tissue. Samples were stored at -80 °C until Quantitative Real-Time RT-PCR (qRT-PCR) was performed.

### Evaluation of the corneal re-epithelialization

The extent of the corneal chemical injury was calculated using the following equation and expressed as a percentage (%):

$$E (\%) = W_s / W_t$$



**Figure 9.** Implantation of PCL fiber into the lower fornix of rat and the sutured eyelids.

Where  $W_s$  is the extent of the cornea stained with fluorescence dye,  $W_i$  is the extent of the whole cornea, and  $E$  represents the ratio indicating the extent of the corneal injury relative to the whole cornea. Denuded epithelium was stained with fluorescein dye, and it was visible under blue LED light. Blue LED light photos of rat corneas following alkali burn were captured on days 0, 1, 2, 3, 4, 7, and 14 after alkali burn. Measurements were processed using NIH ImageJ software (National Institutes of Health, Bethesda, MD, USA). The extent of corneal chemical injury at baseline was assumed to be identical in all three experimental groups and was presented as a percentage (%).

### Evaluation of corneal opacity and neovascularization

The degree of corneal opacity and neovascularization (NV) was measured after administration of 0.1% HA eye drops, crosslinked HA hydrogels, or no treatment to evaluate the efficacy of corresponding treatments. Four clinical researchers (K.S.N., S.K.P., D.R.K. and Y.C.Y) assessed the high-resolution photographs of the cornea and scored the degree of relevant parameters on day 7 post injury using grading measures previously described by Larkin et al<sup>31</sup>. The mean value of two measurements was obtained as a representative value. All data analyses were performed in a manner blinded to treatment groups. Corneal opacity was graded as follows: 0, completely transparent; 1, minimal loss of transparency; 2, moderate loss of transparency but iris vessels visible on retroillumination; 3, iris vessels not visible but pupil outline visible; 4, pupil outline not visible. Corneal neovascularization was graded as follows: 0, no vascularization of graft; 1, vessel growth to 25% of graft radius in any quadrant; 2, vessel growth to 50% of graft radius; 3, vessel growth to 75% of graft radius; 4, vessel growth to center of graft.

### Histological examinations

After completion of the study (on day 7), tissues were isolated. The cornea was carefully separated from the eye while avoiding damage and washed in  $1 \times$  PBS. Tissues were fixed using 4% paraformaldehyde (PFA) solution overnight at 4 °C and then washed in  $1 \times$  PBS. Tissue segments were dehydrated in graded ethanol, embedded in paraffin, and cut into 3- to 4- $\mu$ m-thick sections using a microtome. To study postoperative inflammatory cell infiltration, tissue sections were stained with H & E. To this end, tissue Sects. (3–4  $\mu$ m) were rehydrated by immersing in xylene (3  $\times$  5 min) followed by 100% (twice), 95, 85, and 70% ethanol for 1 min each, deionized water for 1 min, and hematoxylin (BBC Biochemical) and eosin (BBC Biochemical) solutions for 10–20 s before clearing with pure xylene.

### Immunohistochemistry

For immunohistochemistry, tissue Sects. (3–4  $\mu$ m) were rehydrated by immersing in xylene (3  $\times$  5 min), 100% (twice), 95, 85, and 70% ethanol for 5 min each, and deionized water for 5 min. Antigen retrieval buffer (citrate buffer, pH 6.0) was preheated to 92–95 °C. Slides were immersed in the pre-heated solution for 5–10 min. Tissues were encircled with a hydrophobic barrier using a barrier pen. Tissues were further blocked with 2.5% normal horse serum (Vector) for 30 min to 1 h. The slides were washed and incubated with primary antibodies: mouse anti-alpha smooth muscle actin monoclonal antibody (ab7817, Abcam, Cambridge, UK; 1:100 dilution), rabbit IL-1 $\beta$  polyclonal antibody (ab9722, Abcam, Cambridge, UK; 1:1000 dilution), and mouse anti-MMP9 monoclonal antibody (ab58803, Abcam, Cambridge, UK; 1:1000 dilution) at 4 °C overnight. The following day, sections were washed three times in  $1 \times$  PBS followed by incubation with anti-mouse/rabbit IgG secondary antibodies (MP-7500, Vector, Burlingame, CA, USA) at room temperature (20–22 °C) for 1 h in the dark. For the negative controls, nonimmune serum at 1:100 dilution was used instead of the specific primary antibody. After three washes in  $1 \times$  PBS, visualization was performed using a freshly prepared DAB (K5007, DAKO, USA) substrate-chromogen solution for 30–40 s, followed by three washes in  $1 \times$  PBS. Contrast staining was performed using hematoxylin (BBC Biochemical). Sections were observed and imaged with a Trinocular Microscope (Olympus BH2 BHS312, Shinjuku, Tokyo, Japan).

### Western blot analysis

Rat corneal proteins were extracted with cold RIPA buffer (#89900, Thermo Fisher Scientific, USA) with Halt™ Protease and Phosphatase Inhibitor Cocktail (#78441, Thermo Fisher Scientific, USA) and the protein concentration was determined using a protein assay kit (Pierce™ BCA Protein Assay Kit, Thermo Fisher Scientific, USA). Aliquots having equal protein content were subjected to electrophoresis on 10%, 12% Tricine gels and then electrotransferred to PVDF membranes (IPVH00010, Millipore, USA). After a 1-h blocking in 5% Skim milk, the blots were incubated with primary antibodies for: Anti-IL-1 $\beta$  (ab9722, Abcam, UK; 1:1000 dilution), Anti-VEGFA (ab1316, Abcam, UK; 1:1000 dilution), VEGF (MA1-16629, Invitrogen, USA; 1:1000 dilution), TGF $\beta$ 1 (sc-130348, Santa cruz, USA; 1:200 dilution), TGF- $\beta$ 2 (PA5-86215, invitrogen, USA; 1:500 dilution), MK2 (#12155S, Cell Signaling, USA; 1:1000 dilution), and Anti- $\beta$ -Actin (A5441, Sigma, USA; 1:5000 dilution) as a loading control. After washing each membrane three times with Tris-buffered saline containing 1% Tween 20 for 10 min, they were reacted with HRP-conjugated secondary antibodies: anti-rabbit IgG (#7074S, Cell Signaling, USA; 1:3000), anti-mouse IgG (#7076S, Cell Signaling, USA; 1:3000) for 1 h at room temperature, respectively. The specific bands were visualized by an enhanced chemiluminescence reagent (#32132, ECL, Thermo Fisher Scientific, USA) and exposed to Hyperfilm™ ECL™ film (#28906838, Cytiva, USA). The film was developed and the band intensities quantified using ImageJ software (National Institutes of Health, Bethesda, MD, USA).

### Quantitative real-time RT-PCR (qRT-PCR)

The corneas were cut into small pieces and homogenized in TRIzol™ (Invitrogen, #15596018, USA). Briefly, each cornea was immersed in 1 mL of ice-chilled TRIzol and ground with a disposable homogenizer (Biomasher II, #890864; JPN). The concentration of RNA was measured with NanoDrop™ 2000 (Thermo Fisher Scientific,

ND-2000, USA), and 1 µg of RNA templates were used for cDNA synthesis. Generation of cDNA was performed with the reverse transcription reaction kit (PrimeScript™ RT Master Mix, TaKaRa, RR036A; JPN). To determine the gene expression levels, we analyzed 100 ng cDNA with quantitative PCR (qPCR) using the TB Green® Fast qPCR Mix (TaKaRa, RR430A; JPN) based on real-time detection of accumulated fluorescence, in accordance with the manufacturer's instructions (Thermal Cycler Dice Real Time System, Applied, TaKaRa, TP800, JPN). The sequence of primers are as follows: IL-1β (5'-CTGTGACTCGTGGGATGATG-3' and 5'-GGGATTTTGTTCGTTGCTTGT-3'), IL-6 (5'-CACAAGTCCGGAGAGGAGAC-3' and 5'-ACAGTGCATCATCGCTGTTC-3'), GAPDH (5'-GCAAGTCAACGGCACAG-3' and 5'-GCCAGTAGACTCCACGACAT-3'). The amplification program included an initial denaturation step at 95 °C for 30 s, followed by 40 cycles of 95 °C for 5 s, and 60 °C for 10 s, dissociation step 95 °C for 15 s, 60 °C for 30 s, 95 °C for 15 s, after which, a melt curve analysis was conducted to verify amplification specificity. Results were analyzed by the comparative threshold cycle (Ct) method, normalized with GAPDH as an endogenous reference and calibrated against the normal control group.

### Statistical analysis

The statistical significance of differences among groups, including untreated corneas, and corneas treated with DEX eye drops, PCL fibers, and DEX/PCL fibers, was evaluated using one-way analysis of variance (ANOVA) with Tukey's post hoc test, or two way ANOVA with Tukey's post hoc test. *P*-values < 0.05 were considered statistically significant. Data were analyzed using GraphPad Prism 10.2.2 (GraphPad Software, Inc., La Jolla, CA, USA).

### Data availability

Data is provided within the manuscript or supplementary information files.

Received: 18 December 2023; Accepted: 13 May 2024

Published online: 18 September 2024

### References

- Mohan, R. R., Kempuraj, D., D'Souza, S. & Ghosh, A. Corneal stromal repair and regeneration. *Prog. Retin. Eye Res.* **91**, 101090 (2022).
- Nicholas, M. P. & Mysore, N. Corneal neovascularization. *Exp. Eye Res.* **202**, 108363 (2021).
- Gupta, D. & Illingworth, C. Treatments for corneal neovascularization: A review. *Cornea* **30**, 927–938 (2011).
- Lin, A., Patel, N., Yoo, D., DeMartelaere, S. & Bouchard, C. Management of ocular conditions in the burn unit: thermal and chemical burns and Stevens-Johnson syndrome/toxic epidermal necrolysis. *J. Burn Care. Res.* **32**, 547–560 (2011).
- Matsumoto, K. *et al.* Topical betamethasone treatment of stevens-johnson syndrome and toxic epidermal necrolysis with ocular involvement in the acute phase. *Am. J. Ophthalmol.* **253**, 142–151 (2023).
- Shikari, H., Antin, J. H. & Dana, R. Ocular graft-versus-host disease: a review. *Surv. Ophthalmol.* **58**, 233–251 (2013).
- Vaneev, A. *et al.* Nanotechnology for topical drug delivery to the anterior segment of the eye. *Int. J. Mol. Sci.* **22**, 12368 (2021).
- Hosoya, K., Lee, V. H. & Kim, K. J. Roles of the conjunctiva in ocular drug delivery: A review of conjunctival transport mechanisms and their regulation. *Eur. J. Pharm. Biopharm.* **60**, 227–240 (2005).
- Wu, Y. *et al.* Research progress of in-situ gelling ophthalmic drug delivery system. *Asian J. Pharm. Sci.* **14**, 1–15 (2019).
- Jumelle, C., Gholizadeh, S., Annabi, N. & Dana, R. Advances and limitations of drug delivery systems formulated as eye drops. *J. Control Release* **321**, 1–22 (2020).
- Hu, X. *et al.* Electrospinning of polymeric nanofibers for drug delivery applications. *J. Control Release* **185**, 12–21 (2014).
- Shahriar, S. M. S. *et al.* Electrospinning nanofibers for therapeutics delivery. *Nanomaterials (Basel)* **9**, 532 (2019).
- Da Silva, G. R. *et al.* Ocular biocompatibility of dexamethasone acetate loaded poly( $\epsilon$ -caprolactone) nanofibers. *Eur. J. Pharm. Biopharm.* **142**, 20–30 (2019).
- Li, X. *et al.* Supramolecular nanofibers of triamcinolone acetonide for uveitis therapy. *Nanoscale* **6**, 14488–14494 (2014).
- Cejkova, J. *et al.* Treatment of alkali-injured cornea by cyclosporine A-loaded electrospun nanofibers—An alternative mode of therapy. *Exp. Eye Res.* **147**, 128–137 (2016).
- Carter, K. *et al.* Characterizing the impact of 2D and 3D culture conditions on the therapeutic effects of human mesenchymal stem cell secretome on corneal wound healing in vitro and ex vivo. *Acta Biomater* **99**, 247–257 (2019).
- Baskakova, A. *et al.* Electrospun formulations of acyclovir, ciprofloxacin and cyanocobalamin for ocular drug delivery. *Int. J. Pharm.* **502**, 208–218 (2016).
- Cegielska, O., Sierakowski, M., Sajkiewicz, P., Lorenz, K. & Kogermann, K. Mucoadhesive brinzolamide-loaded nanofibers for alternative glaucoma treatment. *Eur. J. Pharm. Biopharm.* **180**, 48–62 (2022).
- Pehlivan, S. B. *et al.* Preparation and in vitro/in vivo evaluation of cyclosporin A-loaded nanodecorated ocular implants for subconjunctival application. *J. Pharm. Sci.* **104**, 1709–1720 (2015).
- Yavuz, B. *et al.* In vivo tissue distribution and efficacy studies for cyclosporin A loaded nano-decorated subconjunctival implants. *Drug Deliv.* **23**, 3279–3284 (2016).
- Singla, J., Bajaj, T., Goyal, A. K. & Rath, G. Development of nanofibrous ocular insert for retinal delivery of fluocinolone acetonide. *Curr. Eye Res.* **44**, 541–550 (2019).
- Gao, H., Gu, Y. & Ping, Q. The implantable 5-fluorouracil-loaded poly(l-lactic acid) fibers prepared by wet-spinning from suspension. *J. Control. Release* **118**, 325–332 (2007).
- Zeng, J. *et al.* Biodegradable electrospun fibers for drug delivery. *J. Control. Release* **92**, 227–231 (2003).
- Zeng, J. *et al.* Influence of the drug compatibility with polymer solution on the release kinetics of electrospun fiber formulation. *J. Control. Release* **105**, 43–51 (2005).
- Dalton, P. D., Lleixà Calvet, J., Mourran, A., Klee, D. & Möller, M. Melt electrospinning of poly-(ethylene glycol-block- $\epsilon$ -caprolactone). *Biotechnol. J.* **1**, 998–1006 (2006).
- Qian, Y., Li, X., Sun, Y., Ke, Q. & Mo, X. Fabrication and characterization of polycaprolactone/chlorophyllin sodium copper salt nanofibrous mats from 2, 2, 2-trifluoroethanol solution by electrospinning. *Iran Polym. J.* **18**, 265–274 (2009).
- Wan, Y., Wu, H., Xiao, B., Cao, X. & Dalai, S. Chitosan-g-polycaprolactone copolymer fibrous mesh scaffolds and their related properties. *Polym. Adv. Technol.* **20**, 795–801 (2009).
- Yang, K., Park, S., Choi, Y. & Cho, C. Fiber formation from semi-interpenetrating polymer networks consisting of polycaprolactone and a poly (ethylene glycol) macromer. *J. Appl. Polym. Sci.* **84**, 835–841 (2002).
- Hersh, P. S. *et al.* Topical nonsteroidal agents and corneal wound healing. *Arch. Ophthalmol.* **108**, 577–583 (1990).
- Ryu, J. S., Ko, J. H., Kim, M. K., Wee, W. R. & Oh, J. Y. Prednisolone induces apoptosis in corneal epithelial cells through the intrinsic pathway. *Sci. Rep.* **7**, 4135 (2017).

31. Srinivasan, B. D. Corneal reepithelialization and anti-inflammatory agents. *Trans. Am. Ophthalmol. Soc.* **80**, 758–822 (1982).
32. Larkin, D. F., Calder, V. L. & Lightman, S. L. Identification and characterization of cells infiltrating the graft and aqueous humour in rat corneal allograft rejection. *Clin. Exp. Immunol.* **107**, 381–391 (1997).
33. Dana, M. R., Zhu, S. N. & Yamada, J. Topical modulation of interleukin-1 activity in corneal neovascularization. *Cornea* **17**, 403–409 (1998).
34. BenEzra, D., Hemo, I. & Maftzir, G. In vivo angiogenic activity of interleukins. *Arch. Ophthalmol.* **108**, 573–576 (1990).
35. Fukuda, M., Mishima, H. & Otori, T. Detection of interleukin-1 beta in the tear fluid of patients with corneal disease with or without conjunctival involvement. *Jpn. J. Ophthalmol.* **41**, 63–66 (1997).
36. Nakao, S. *et al.* Dexamethasone inhibits interleukin-1beta-induced corneal neovascularization: role of nuclear factor-kappaB-activated stromal cells in inflammatory angiogenesis. *Am. J. Pathol.* **171**, 1058–1065 (2007).
37. Calienno, R., Curcio, C., Lanzini, M., Nubile, M. & Mastropasqua, L. In vivo and ex vivo evaluation of cell-cell interactions, adhesion and migration in ocular surface of patients undergone excimer laser refractive surgery after topical therapy with different lubricant eyedrops. *Int. Ophthalmol.* **38**, 1591–1599 (2018).
38. Ghasemi, H. Roles of IL-6 in ocular inflammation: A review. *Ocul. Immunol. Inflamm.* **26**, 37–50 (2018).
39. Baggolini, M. & Clark-Lewis, I. Interleukin-8, a chemotactic and inflammatory cytokine. *FEBS Lett.* **307**, 97–101 (1992).
40. Ebihara, N., Ohtomo, K., Tokura, T., Ushio, H. & Murakami, A. Effect of tacrolimus on chemokine production by corneal myofibroblasts via toll-like receptors, compared with cyclosporine and dexamethasone. *Cornea* **30**, 702–708 (2011).
41. Wang, S., Liu, R., Fu, Y. & Kao, W. J. Release mechanisms and applications of drug delivery systems for extended-release. *Expert Opin. Drug Deliv.* **17**, 1289–1304 (2020).
42. Chang, H. I., Lau, Y. C., Yan, C. & Coombes, A. G. Controlled release of an antibiotic, gentamicin sulphate, from gravity spun polycaprolactone fibers. *J. Biomed. Mater. Res. A* **84**, 230–237 (2008).
43. Luong-Van, E. *et al.* Controlled release of heparin from poly(epsilon-caprolactone) electrospun fibers. *Biomaterials* **27**, 2042–2050 (2006).
44. Sandor, M., Ensore, D., Weston, P. & Mathiowitz, E. Effect of protein molecular weight on release from micron-sized PLGA microspheres. *J. Control. Release* **76**, 297–311 (2001).
45. Peng, R. *et al.* The PEG-PCL-PEG hydrogel as an implanted ophthalmic delivery system after glaucoma filtration surgery; A pilot study. *Med. Hypothesis Discov. Innov. Ophthalmol.* **3**, 3–8 (2014).
46. Da Silva, G. R. *et al.* In vitro and in vivo ocular biocompatibility of electrospun poly(epsilon-caprolactone) nanofibers. *Eur. J. Pharm. Sci.* **73**, 9–19 (2015).

## Acknowledgements

This study was supported by a grant from the National Research Foundation of Korea (NRF) (2022R1A2C2006109, 2021R1A6A1A03038996). The sponsor or funding organization had no role in the design or conduct of this research.

## Author contributions

Study concept and design: D.R.K., S.K.P., E.J.K., K.S.N Acquisition, analysis, or interpretation of data: D.R.K., S.K.P., E.J.K., D.K.K., K.S.N Drafting of the manuscript: D.R.K., S.K.P., K.S.N Critical revision of the manuscript for important intellectual content: D.R.K., S.K.P., E.J.K., D.K.K., Y.C.Y, K.S.N, D.M., H.J.L Administrative, technical or material support : E.J.K., D.M., H.J.L Study supervision: K.S.N Funding acquisition : K.S.N

## Competing interests

The authors declare that they have no known competing financial interests or personal relationships that could have appeared to influence the work reported in this paper.

## Additional information

**Supplementary Information** The online version contains supplementary material available at <https://doi.org/10.1038/s41598-024-62026-x>.

**Correspondence** and requests for materials should be addressed to H.J.L. or K.-S.N.

**Reprints and permissions information** is available at [www.nature.com/reprints](http://www.nature.com/reprints).

**Publisher's note** Springer Nature remains neutral with regard to jurisdictional claims in published maps and institutional affiliations.

**Open Access** This article is licensed under a Creative Commons Attribution-NonCommercial-NoDerivatives 4.0 International License, which permits any non-commercial use, sharing, distribution and reproduction in any medium or format, as long as you give appropriate credit to the original author(s) and the source, provide a link to the Creative Commons licence, and indicate if you modified the licensed material. You do not have permission under this licence to share adapted material derived from this article or parts of it. The images or other third party material in this article are included in the article's Creative Commons licence, unless indicated otherwise in a credit line to the material. If material is not included in the article's Creative Commons licence and your intended use is not permitted by statutory regulation or exceeds the permitted use, you will need to obtain permission directly from the copyright holder. To view a copy of this licence, visit <http://creativecommons.org/licenses/by-nc-nd/4.0/>.

© The Author(s) 2024